THE JOURNAL OF PHYSICAL CHEMISTRY B

Article

pubs.acs.org/JPCB

# Electron Attachment to the Guanine–Cytosine Nucleic Acid Base Pair and the Effects of Monohydration and Proton Transfer

Ashutosh Gupta,[†] Heather M. Jaeger,[‡] Katherine R. Compaan,[§] and Henry F. Schaefer, III*[,§]

[†]Udai Pratap Autonomous College, Varanasi 221002, India

[‡]Department of Chemistry, University of Rochester, Rochester, New York 14614, United States

[§]Center for Computational Quantum Chemistry, University of Georgia, Athens, Georgia 30602, United States

Supporting Information

**ABSTRACT:** The guanine–cytosine (GC) radical anion and its interaction with a single water molecule is studied using ab initio and density functional methods. Z-averaged second-order perturbation theory (ZAPT2) was applied to GC radical anion for the first time. Predicted spin densities show that the radical character is localized on cytosine. The Watson–Crick monohydrated GC anion is compared to neutral GC·$H_2O$, as well as to the proton-transferred analogue on the basis of structural and energetic properties. In all three systems, local minima are identified that correspond to water positioned in the major and minor grooves of macromolecular DNA. On the anionic surface, two novel structures have water positioned above or below the GC plane. On the neutral and anionic surfaces, the global minimum can be described as water interacting with the minor groove. These structures are predicted to have hydration energies of 9.7 and 11.8 kcal $mol^{-1}$, respectively. Upon interbase proton-transfer (PT), the anionic global minimum has water positioned in the major groove, and the hydration energy increases to 13.4 kcal $mol^{-1}$. PT GC·$H_2O^{\bullet-}$ has distonic character; the radical character resides on cytosine, while the negative charge is localized on guanine. The effects of proton transfer are further investigated through the computed adiabatic electron affinities (AEA) of GC and monohydrated GC, and the vertical detachment energies (VDE) of the corresponding anions. Monohydration increases the AEAs and VDEs by only 0.1 eV, while proton-transfer increases the VDEs substantially (0.8 eV). The molecular charge distribution of monohydrated guanine–cytosine radical anion depends heavily on interbase proton transfer.

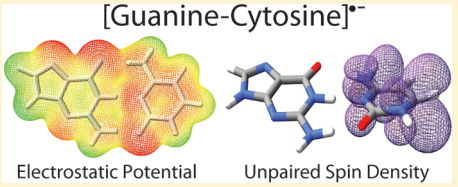


## INTRODUCTION

Nucleic acid bases (NABs) in DNA are responsible for the storage and processing of genetic information. Exposure to high-energy radiation can damage and mutate DNA, leading to cellular senescence, programmed cell death, or carcinogenesis. The physiological manifestations of DNA damage include aging, neurological syndromes, and cancer. DNA damage mechanisms often include ionization events, which result in charged base radicals.[1,2] These radicals are produced by way of direct or indirect mechanisms.[3−8] Direct DNA damage is one-electron oxidation due to irradiation of the base itself, and indirect damage occurs by way of secondary species generated by the ionizing radiation, including $OH^{\bullet}$, $O_2^{\bullet-}$, and $H_2O_2$. In addition to these molecular species, the radiolysis of water gives rise to damaging, low-energy electrons (LEE)[9] that can attach to NABs.[10,11] Ionization events in and around DNA have implications beyond DNA damage. The formation of radicals in DNA fragments is an important step in many biochemical processes such as DNA repair,[12−16] charge transfer,[17,18] cascading ionization,[12,13] and electron transport.[16,19,20]

Reductive damage to single- and double-stranded DNA by LEE[21] has inspired numerous studies on electron attachment to various DNA fragments.[22−24] Specifically, the attachment of low-energy electrons has been shown to induce strand breaks in single-strand DNA.[25−28] Reduced NABs, formed by electron trapping, play a significant role in indirect DNA damage.[15,17,29,30]

The lifetime of a reduced NAB can be understood in terms of the electron affinity of the neutral species; longer-lived anionic species have larger electron affinities. Thus, electron affinities of NABs provide a quantitative measure of the relative importance of ionized intermediates in DNA damage pathways. NABs with larger adiabatic and vertical electron affinities (AEAs and VEAs) hold extra electrons more easily. Therefore, they play a more significant role in the chemical processes that lead to mutation and damage of DNA. Electron affinities of individual NABs have been studied using second-order Møller-Plesset perturbation theory (MP2),[31] coupled-cluster with single, double, and perturbative triple excitations [CCSD(T)],[32−37] semiempirical methods,[38] and density functional theory (DFT).[31,39,40] The largest NAB EA was reported for uracil, followed by thymine and cytosine.[40] As a further step toward understanding electron attachment to DNA, EAs have been computed for Watson–Crick base pairs[41−46] and even nucleosides[47] using DFT. Watson–Crick base pairs[48] have also been studied at the MP2 level of theory.

**Received:** December 2, 2011
**Revised:** April 16, 2012
**Published:** April 24, 2012





dx.doi.org/10.1021/jp211608b | J. Phys. Chem. B 2012, 116, 5579–5587

Theoretical work is complemented by extensive experimental investigations on the attachment of low-energy electrons to DNA. Gas-phase electron affinities of DNA fragments have been measured using photoelectron spectroscopy,[49−53] electron transmission spectroscopy,[54] Rydberg electron-transfer (RET) spectroscopy,[55,56] and electron attachment spectroscopy.[57−59] Furthermore, electron attachment to NABs has been studied in low-temperature LiCl glasses with electron spin resonance (ESR) spectroscopy.[60] Under certain experimental conditions, DNA base pairs and methylated DNA base pairs undergo interbase proton transfer (PT) upon electron attachment.[61−63]

Electron attachment typically engenders proton transfer in DNA to produce distonic species:[64,65] that is, species with charge and radical characters spatially separate. Proton transfer influences mutation pathways,[66,67] charge transport along DNA,[68−70] and direct DNA damage[71−76] as a result of the electronic changes upon isomerization. A recent review covers the mechanistic details of proton-coupled electron transfer.[77] Furthermore, PT has a large effect on an NAB pair's ability to support a negative charge. For instance, the theoretical VDE of proton-transferred $[GC]^-$ is 2.1 eV,[41] while VEAs of the Watson−Crick base pairs are less than 1.0 eV.[44,45] DFT studies have shown that the proton-transferred isomer of the guanine−cytosine radical anion is lower in energy than the canonical structure.[41,78] The guanine−cytosine base pair is unique in this regard since $[AT]^-$ does not exhibit stabilization upon interbase proton transfer.[42]

Hydration effects on the electron affinities of NABs must be accounted for in order to build an accurate picture of DNA ionization and the subsequent damage mechanisms. In bulk water, the structure of DNA, as well as individual NAB structures, differ from those in the gas phase.[79−83] The nature of the ionizing electron, i.e., dipole-bound vs valence-bound, of NAB radical anions depends on the presence of solvating water molecules, according to photoelectron spectroscopy.[50] SCF and DFT studies have shown that electron attachment is energetically more favorable for explicity microsolvated NABs than for isolated NABs.[84−91]Refining this picture further, Schiedt and co-workers demonstrated that the EAs of uracil, thymine, and cytosine depend linearly on the number of surrounding water molecules.[51] Finally, proton transfer, which is intertwined with electron attachment, is facilitated by hydration at certain sites in both the GC radical anion[92] and the methylated GC radical anion.[93]

In the present work, structures and interaction energies are reported for the neutral GC base pair as well as for the GC radical anion ($[GC]^{\bullet-}$). The electrostatic potential (ESP) gives evidence for strong water−base interactions around the periphery of the base pair. We explore the effects of electron attachment on the hydration structure through theoretical structures and hydration energies of both neutral and anionic GC monohydrates ($GC{\cdot}H_2O$). The spatial distribution of radical character is shown by the spin density. Molecular charge distributions are computed to demonstrate the effects of noncovalent interactions and interbase proton transfer. Changes in electronic properties due to PT are demonstrated through adiabatic electron affinities and vertical detachment energies of the Watson−Crick structures compared to the proton-transferred species. We show that the lowest energy trimer arises from distonic interbase proton transfer and interaction of water within the major groove.

## THEORETICAL METHODS

All stationary point structures were found using unrestricted Kohn−Sham density functional theory (DFT), namely, with the B3LYP functional.[94,95] All nuclear degrees of freedom were optimized, yielding fully relaxed structures. A double-$\zeta$ quality basis set[96−98] (DZP++), having proven reliable in similar applications,[40,44,45,47,72,86,99] was employed for all DFT calculations.

The integration quadrature grid consisted of 75 radial shells with 302 angular points per shell. In order to classify the stationary points as minima or transition states (TS), harmonic vibrational frequencies were computed via analytic second derivatives. The computed frequencies were also used to provide an estimate of the zero-point vibrational energy (ZPVE).

Given the many nuclear degrees of freedom of monohydrated GC, the search for minima and transition states on the potential energy surface (PES) was necessarily carried out in a systematic manner. We utilized the fact that a strong charge−dipole interaction exists between water and charged DNA bases[100,101] and directed the positive end of water's dipole moment toward the base. Initial geometries were generated by systematically placing a water molecule around the Watson−Crick GC anion, coplanar with the NABs. Additional starting structures were considered in which water sits above the GC base pair. A total of 30 initial geometries were optimized, none of which resulted in planar structures.

Interaction energies of the Watson−Crick guanine−cytosine base pair were computed with both B3LYP/DZP++ and Z-averaged second-order perturbation theory[102−105] (ZAPT2)/aug-cc-pVDZ methods. The ZAPT2 results should be more accurate than DFT or MP2 results on the GC radical anion system.[106] Dunning's correlation-consistent aug-cc-pVDZ[107,108] basis set contains the diffuse functions necessary to model noncovalent interactions and *d*-polarization functions, which are important for the computation of hydrogen bonding energies.[109] Interaction energies ($\Delta E_{WC}$) were computed by way of the following supramolecular approach:

$$\Delta E_{WC} = E_{GC^-} - E_G - E_{C^-} \quad (1)$$

where $E_{GC^-}$ is the energy of GC radical anion; $E_G$ is the energy of neutral guanine; and $E_{C^-}$ is the energy of cytosine radical anion. The interaction energies for proton-transferred radical anions ($\Delta E_{PT-WC}$) were computed as follows:

$$\Delta E_{PT-WC} = E_{PT-GC^-} - E_{G-H^-} - E_{C+H} \quad (2)$$

where, in this case, $E_{PT-GC^-}$ is the energy of the PT GC radical anion, while $E_{G-H^-}$ is the energy of guanine anion with a hydrogen removed from N1. Finally, $E_{C+H}$ is the energy of cytosine with an extra hydrogen on N3. The counterpoise-correction was not applied since it does not always improve the accuracy of MP2 hydrogen bond interaction energies with modestly sized basis sets.[110]

Hydration energies, $\Delta E_{HYD}$, were computed at the B3LYP/DZP++ and ZAPT2/aug-cc-pVDZ levels of theory in a similar, supramolecular fashion

$$\Delta E_{HYD} = E_{GCW^-} - E_{GC^-} - E_W \quad (3)$$

where $E_{GCW^-}$ is the energy of the trimer; $E_{GC^-}$ is the energy of GC anion; and $E_W$ is the energy of the water monomer. All energies on the right-hand-sides of eqs 1 and 2 were evaluated at the equilibrium geometries of the isolated species.


dx.doi.org/10.1021/jp211608b | J. Phys. Chem. B 2012, 116, 5579−5587

ZPVE corrections were calculated by including the B3LYP/DZP++ ZPVE for each isolated species prior to computing the hydration energies at the ZAPT2/aug-cc-pVDZ level of theory. The magnitude of the hydration energies dictates the energetic ordering of $[GC{\cdot}H_2O]^{\bullet-}$, such that the structure with the largest ZPVE-corrected hydration energy is the global minimum.

The electronic properties of each structure were investigated through charge distributions and spin densities, as well as through electron affinities and detachment energies. Charge distributions were determined using natural bond orbital (NBO) partial atomic charges[111−115] based on the B3LYP/DZP++ electron density. The fraction of negative charge associated with each monomer was calculated as the sum of all the atomic charges in that monomer. Likewise, spin densities, which reflect the spatial distribution of the unpaired electron, were computed at the B3LYP/DZP++ level of theory. VEAs were computed as the energy difference between anion and neutral at the optimized neutral geometry. The AEA is the energy difference between the opimized anion and the optimized neutral. Finally, the VDEs were computed by subtracting the neutral energy from the anion energy, both at the equilibrium geometry of the anion. All computations were carried out using the QChem 3.2 package.[116]

## RESULTS AND DISCUSSION

Electron attachment to GC monohydrate produces a strongly interacting cluster consisting of guanine, cytosine radical anion, and water.

This investigation of the physical nature of the ionized products begins with isolated GC, continues to the interaction with a single water molecule, and ends with interbase proton transfer. The first two steps are representative of the initial kinetic product formed upon ionization. Proton-transferred species are representative of thermal ionization products. The computed physical properties, including structure, hydration energy, spin density, charge distribution, and electron affinities of $[GC{\cdot}H_2O]^{\bullet-}$ contribute to our understanding of direct DNA damage.

**Watson−Crick GC Base Pair.** Figure 1 shows the atomic labeling scheme employed for the GC base pair in the Watson−Crick conformation. Both oxidation and reduction of GC lead to similar distortions of the interbase hydrogen-bond network. Table 1 lists the structural features of the cationic, neutral, and anionic base pairs. The hydrogen bond lengths involving N−H moieties of guanine are shorter in charged species than in neutral GC. However, the hydrogen bond formed by the cytosine amino group becomes significantly stretched in the anion and cation, compared to the neutral species. Regardless of whether GC is oxidized or reduced, the Watson−Crick conformation distorts, widening one region of the hydrogen-bond network. Upon oxidation, the hole is delocalized over guanine,[100] while cytosine carries the additional electron upon reduction. (See spin density discussion below.) Distinct from the neutral and the cation, GC anion is nonplanar. This nonplanarity arises from both an out-of-plane twist defined by the G(N10)−G(N1)−C(N3)−C(O7) dihedral angle and a slight pyrimidalization of the G(N10) amino group. These ionization-induced structural changes are associated with disruption of the GC hydrogen bonds.

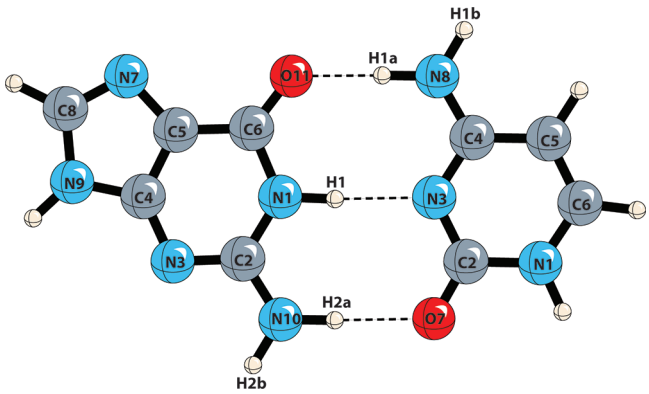


**Figure 1.** Qualitative structure for the guanine−cytosine base pair. (Guanine is shown on the left.) This atomic labeling scheme is used throughout the text.

**Table 1. Structural Features of the Guanine−Cytosine Neutral, Cation, and Anion[a]**

| | cation | neutral | anion |
|---|---|---|---|
| G(O11)·C(H1a) | 1.93 | 1.72 | 1.98 |
| G(H1)·C(N3) | 1.76 | 1.89 | 1.76 |
| G(H2a)·C(O7) | 1.60 | 1.88 | 1.65 |
| interbase dihedral | 0.0 | 0.0 | 15.4 |
| amino pyramidalization | 0.0 | 0.0 | 4.6 |

[a]Equilibrium geometries were computed at the B3LYP/DZP++ level of theory. Hydrogen-bond distances are given in Å. The interbase twist angle is defined as the dihedral angle formed by atoms G(N10)−G(N1)−C(N3)−C(O7) (Figure 1). The pyramidalization angle is defined as the out-of-plane bend of the two amino atoms. Units for angles are degrees.

Interaction energies ($\Delta E_{WC}$) for GC, $[GC]^{\bullet+}$, and $[GC]^{\bullet-}$ are reported in Table 2. In addition, $\Delta E_{WC}$ values are provided for proton-transferred (PT) $[GC]^{\bullet-}$ in which G(H1) has transferred to the cytosine moiety. The interaction energy of the charged GC base pairs is significantly larger than the interaction energy of the neutral. At first glance, the simultaneous increase in interaction energy and distortion of the strong hydrogen-bond network upon ionization seem contradictory. However, the charge−dipole interaction between adjacent NABs is much stronger than local hydrogen bonds. In the Watson−Crick structure, this charge−dipole interaction is attractive. Therefore, the relative orientations of the ionized NABs are slightly altered through small perturbations in the interbase hydrogen bonds. At the same time, ionization increases the interaction strength.

**Table 2. Interaction Energies of the Neutral Guanine−Cytosine (GC) Base Pair, GC Radical Cation, GC Radical Anion, and the Proton-Transferred Conformation of GC Radical Anion, As Defined in Eqs 1 and 2[a]**

| | ZAPT2/aug-cc-pVDZ | B3LYP/DZP++ |
|---|---|---|
| GC | 30.3 (28.5) | 27.2 (25.4) |
| $[GC]^{\bullet+}$ | 49.2 (46.9) | 45.1 (43.2) |
| $[GC]^{\bullet-}$ | 42.7 (41.7) | 39.5 (38.5) |
| PT $[GC]^{\bullet-}$ | 32.6 (31.6) | 29.6 (28.7) |

[a]Energies are reported in kcal $mol^{-1}$. ZPVE-corrected values are displayed in parentheses.

As mentioned at the start of this section, the unpaired electron of $[GC]^{\bullet-}$ is delocalized over the $\pi$-system of cytosine. Figure 2 shows the B3LYP/DZP++ spin density of $[GC]^{\bullet-}$,


dx.doi.org/10.1021/jp211608b | J. Phys. Chem. B 2012, 116, 5579−5587

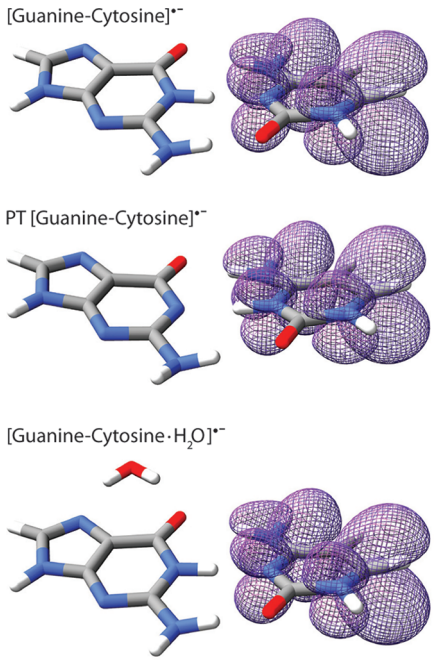


**Figure 2.** Spin density computed at the B3LYP/DZP++ level of theory. The top panel shows the GC radical anion, $[GC]^{\bullet-}$, in the Watson−Crick configuration. The middle panel shows the spin density upon the G(N1)−H1·C(N3) proton transfer. The bottom panel displays the spin density of $[GC]^{\bullet-}$ in the presence of a single water molecule.

$[GC{\cdot}H_2O]^{\bullet-}$, and proton-transferred GC radical anion (PT $[GC]^{\bullet-}$). Adiabatic electron affinities of the individual NABs show variances depending on the theoretical method employed, but cytosine consistently has a more positive AEA than guanine,[40] which is in agreement with the computed spin density. Neither the interaction with a single water molecule nor interbase proton transfer affects the spatial extent of the unpaired electron. Computed AEAs of GC range from 0.28 to 0.99 eV.[41,44,84] At the B3LYP/DZP++ level of theory, the AEA of GC is computed to be 0.44 eV. Given that previous theoretical estimates of the AEA of cytosine were either negative or slightly positive, the interbase interaction lowers the energy of the radical anion. Monohydration of the base pair further increases the AEA by an additional 0.16 eV. Thus, although water and guanine do not carry significant spin in the $[GC{\cdot}H_2O]^{\bullet-}$ complex, their presence facilitates electron attachment.

The ESPs of GC in its neutral and anionic states are shown in Figure 3. Upon electron attachment, the ESP becomes more negative (shades of red) over both guanine and cytosine. Proton transfer induces a small, local change in the ESP near the central hydrogen bond. Water feels the PT $[GC]^{\bullet-}$ generated ESP, which is most negative near the oxygen atoms of cytosine and guanine. In PT $[GC]^{\bullet-}$, the ESP does not follow the spin density because the spatial distribution of the radical electron and the negative regions of the ESP do not entirely coincide. As a result, water will not preferentially interact with the cytosine moiety in PT $[GC]^{\bullet-}$. Hydration sites correspond to negative regions of the ESP, and the positive end of water's dipole moment is directed toward the base pair.

**GC Monohydrates.** The structures of GC monohydrates can be classified according to the water molecule's orientation

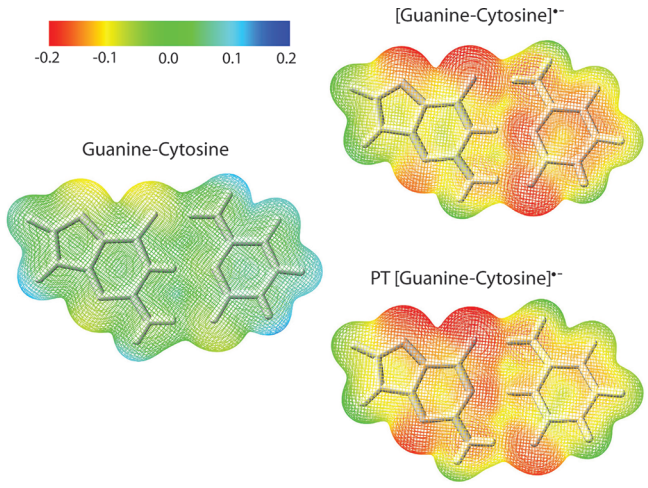


**Figure 3.** Electrostatic potential (ESP) of the neutral, radical anion, and proton-transferred radical anion structures of guanine−cytosine. Values of the ESP are in atomic units.

with respect to macromolecular DNA. Both the anionic and neutral trimers exhibit minima in which water binds to DNA in the major groove, the minor groove, and the stack. The stack is here defined to be the region above and below the GC plane. Although the hydration sites are similar in the neutral and anionic forms of $GC{\cdot}H_2O$, the orientations of water at these sites typically differ. A total of six minima are identified for $[GC{\cdot}H_2O]^{\bullet-}$, and five minima are identified for $GC{\cdot}H_2O$.

Structures corresponding to water interacting within the major groove are shown in Figure 4. Interestingly, direct comparison of structure **1** on the neutral surface to anionic $\mathbf{1}^{\bullet-}$

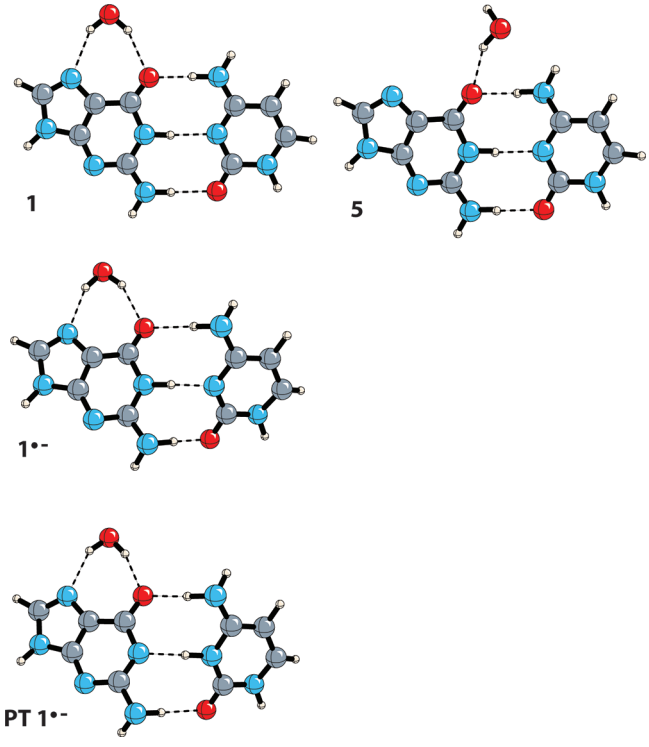


**Figure 4.** Structures of neutral and anionic $GC{\cdot}H_2O$ in which water interacts within the major groove. Monohydrated structures on the left show a similar hydration site on guanine for GC, $[GC]^{\bullet-}$, and proton-transferred $[GC]^{\bullet-}$.


dx.doi.org/10.1021/jp211608b | J. Phys. Chem. B 2012, 116, 5579−5587

reveals very little structural dependence on ionization. On either surface, both hydrogen atoms of water form hydrogen bonds. The hydrogen bond lengths of G(N7)·HOH and G(O11)·HOH are slightly shorter (by <0.05 Å) in the anion. The fact that water in the major groove does not reorient upon electron attachment cannot be attributed to a lack of charge–dipole interaction. The ESP of $[GC]^{\bullet-}$ (Figure 3) clearly shows that the space around guanine is strongly influenced by ionization. Structure **5** of the neutral trimer is also a major groove hydrate. It has a larger hydration energy than structure **1** and involves a cooperative interaction between water, G(O11), and the C(N8) amino group. An equivalent anionic equilibrium structure does not exist.

Minor groove hydrates arise from the strong attraction of water to sites near C(O7) and G(N3), as seen in Figures 5 and 6, respectively. Three minor groove minima were located on the $[GC{\cdot}H_2O]^{\bullet-}$ potential energy surface, namely, $\mathbf{2}^{\bullet-}$, $\mathbf{3}^{\bullet-}$, and $\mathbf{4}^{\bullet-}$. Three similar structures, **2**, **3**, and **4**, were identified for the neutral system. All structures, regardless of charge state, involve a hydrogen atom of water directed either above or below the GC plane. Water forms a single hydrogen bond with C(O7) in $\mathbf{2}^{\bullet-}$ and $\mathbf{3}^{\bullet-}$. In the neutral analogues, the hydrogen bonds are slightly longer. Unlike the minor groove minima of $[GC{\cdot}H_2O]^{\bullet-}$, the neutral minor groove $GC{\cdot}H_2O$ structures contain cooperative hydrogen bonds. Structures **2** and **3** involve cooperative hydrogen bonds between water and cytosine, while **4** contains cooperative hydrogens bonded between water and guanine. Anionic structures $\mathbf{2}^{\bullet-}$, $\mathbf{3}^{\bullet-}$, and $\mathbf{4}^{\bullet-}$ involve the same hydration sites as the neutral systems, but a single hydrogen bond is formed. The interaction of water in the minor groove is structurally distinct between neutral and anionic systems. The difference arises from the strong charge-dipole interaction that overwhelms the delicate intermolecular potential, negating the feasibility of cooperative hydrogen bonding.

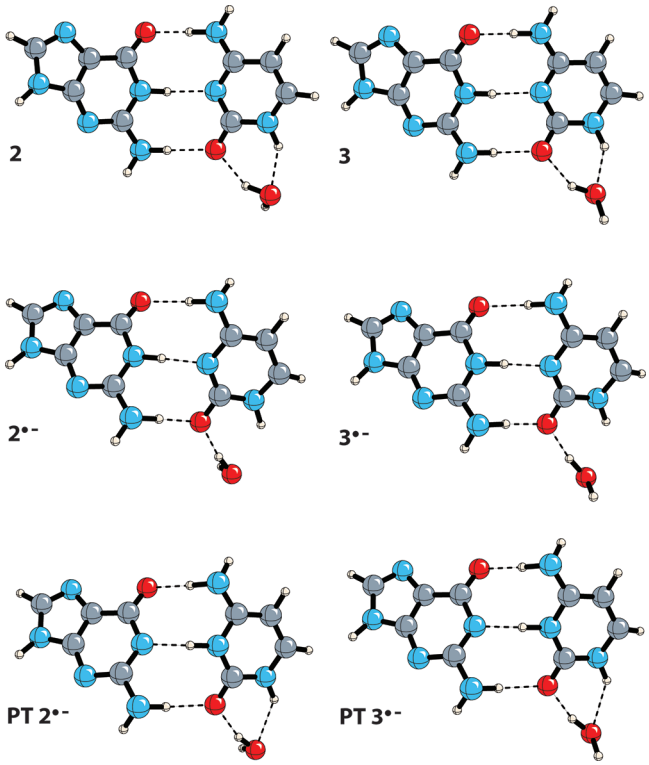


**Figure 5.** Minor groove structures of monohydrated GC, $[GC]^{\bullet-}$, and proton-transferred $[GC]^{\bullet-}$. Structures **2** and **3** correspond to water interacting with cytosine, whereas the minor groove structures of **4** (Figure 6) show water interacting with guanine. Note that structures **2** and **3** only differ in the orientation of water relative to the GC plane.

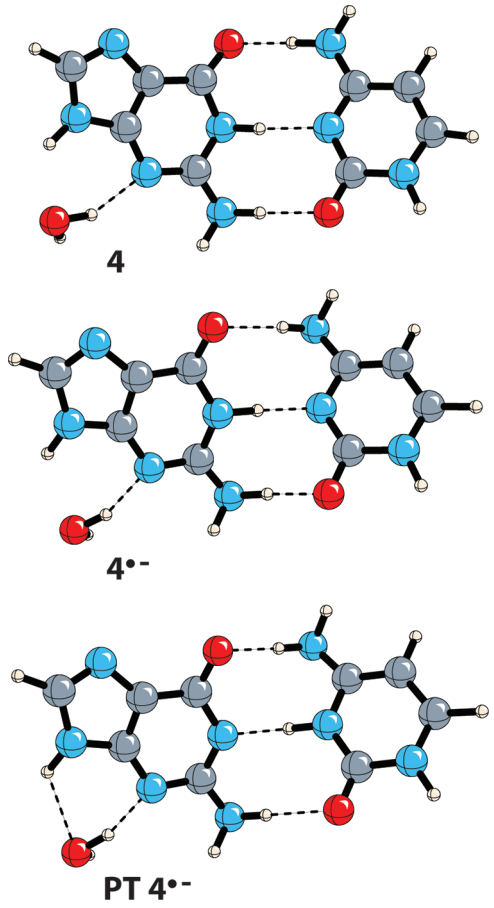


**Figure 6.** Minor groove structures of $GC{\cdot}H_2O$, $GC{\cdot}H_2O$ radical anion, and PT $GC{\cdot}H_2O$ radical anion resulting from the G(N1)–H1 to C(N3) proton transfer, in order from top to bottom. Water interacts with guanine.

In ionized $GC{\cdot}H_2O$, water can also bind to the GC plane from above or below. These structures are classified as stack hydrates. (The GC plane should be interpreted loosely since the base pair is slightly nonplanar.) The two stack hydrates of $[GC{\cdot}H_2O]^{\bullet-}$ are displayed in Figure 7. Water hovers close to G(O11) and C(N8) in structure $\mathbf{5}^{\bullet-}$, and both of water's hydrogen atoms are directed toward the base pair. In structure $\mathbf{6}^{\bullet-}$, water forms a single hydrogen bond with C(N8). The stack hydrates result from a charge–dipole interaction that is easily captured with standard DFT methods and suggest a intercalation pathway not available to the neutral species.

Table 3 provides the monohydration energies of both neutral and anionic GC. The ZPVE-corrected values give the best estimates of $\Delta E_{HYD}$. However, comparison of $\Delta E_{HYD}$ at the uncorrected B3LYP and ZAPT2 levels of theory provides additional insight. $\Delta E_{HYD}$ computed at the B3LYP level indicates that structure $\mathbf{1}^{\bullet-}$ is the global minimum, with $\mathbf{2}^{\bullet-}$, $\mathbf{3}^{\bullet-}$, and $\mathbf{4}^{\bullet-}$ being less than 0.6 kcal mol$^{-1}$ higher in energy. This is in agreement with the MP2 results. Since structures $\mathbf{1}^{\bullet-}$, $\mathbf{4}^{\bullet-}$, and $\mathbf{5}^{\bullet-}$ involve guanine–water interactions, there is no energetic benefit to solely hydrating the unpaired electron on cytosine. The stack structures ($\mathbf{5}^{\bullet-}$ and $\mathbf{6}^{\bullet-}$) are about 2.0 kcal mol$^{-1}$ higher in energy than the groove structures. Structures **2**


dx.doi.org/10.1021/jp211608b | J. Phys. Chem. B 2012, 116, 5579–5587

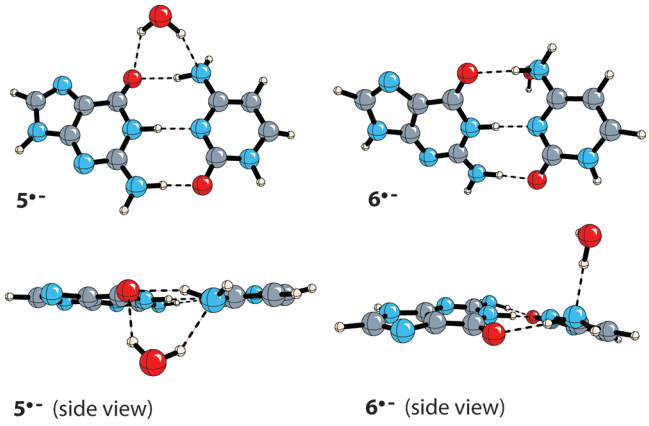


**Figure 7.** Stack structures of monohydrated $GC^{\bullet-}$. The left panel displays top and side views of water interacting above the plane of the GC. On the right-hand side, $\mathbf{6}^{\bullet-}$, water approaches the top plane of GC near cytosine.

**Table 3. Monohydration Energies of Neutral GC, the GC Radical Anion, and the Proton-Transferred Conformation of the GC Radical Anion, at the Hartree–Fock (HF), B3LYP, and ZAPT2 Levels of Theory[a]**

| | HF | correlation | B3LYP(B3LYP) | ZAPT2(B3LYP) |
|---|---|---|---|---|
| | | Neutral | | |
| major groove | | | | |
| **1** | 6.6 | 3.6 | 9.4 (7.1) | 10.2 (7.9) |
| **5** | 7.5 | 2.7 | 9.1 (7.5) | 10.2 (8.3) |
| minor groove | | | | |
| **2** | 7.3 | 4.7 | 11.1 (8.7) | 12.1 (9.7) |
| **3** | 7.3 | 4.7 | 11.1 (8.7) | 12.1 (9.7) |
| **4** | 6.1 | 5.6 | 10.1 (7.8) | 11.8 (8.3) |
| | | Anionic | | |
| major groove | | | | |
| $\mathbf{1}^{\bullet-}$ | 9.1 | 4.7 | 13.2 (11.0) | 13.9 (11.6) |
| minor groove | | | | |
| $\mathbf{2}^{\bullet-}$ | 9.2 | 4.2 | 12.9 (10.7) | 13.4 (11.2) |
| $\mathbf{3}^{\bullet-}$ | 9.2 | 4.2 | 12.9 (10.6) | 13.4 (11.1) |
| $\mathbf{4}^{\bullet-}$ | 7.7 | 6.3 | 12.6 (10.4) | 14.0 (11.8) |
| stack | | | | |
| $\mathbf{5}^{\bullet-}$ | 7.9 | 3.8 | 11.3 (9.0) | 11.8 (9.5) |
| $\mathbf{6}^{\bullet-}$ | 6.6 | 5.0 | 11.0 (9.1) | 11.6 (9.7) |
| | | Proton-Transferred | | |
| major groove | | | | |
| **PT** $\mathbf{1}^{\bullet-}$ | 11.9 | 4.2 | 15.5 (12.8) | 16.1 (13.4) |
| minor groove | | | | |
| **PT** $\mathbf{2}^{\bullet-}$ | 7.4 | 5.4 | 11.7 (9.5) | 12.8 (10.6) |
| **PT** $\mathbf{3}^{\bullet-}$ | 7.5 | 5.1 | 11.7 (9.4) | 12.6 (10.4) |
| **PT** $\mathbf{4}^{\bullet-}$ | 9.2 | 5.6 | 13.8 (11.5) | 14.9 (12.5) |

[a]Correlation contributions to binding energies are obtained from the ZAPT2 results. Energies are in units of kcal $mol^{-1}$. ZPVE-corrected values are indicated in parentheses.

and **3** are nearly isoenergetic; they represent the global minima of $GC{\cdot}H_2O$ and have water positioned in the minor groove. The hydration energy of the neutral system in the global minimum configuration is 9.7 kcal $mol^{-1}$, indicating a strong hydrogen bond. Both B3LYP and ZAPT2 yield the correct energetic ordering of the neutral structures when the ZPVE is included. The electronic correlation contribution to $\Delta E_{HYD}$ of the minor groove neutral structures is larger than in the major groove neutral structures by more than 1.0 kcal $mol^{-1}$, indicating the importance of correlation in cooperative hydrogen bonds.

Along with nontrivial structural changes, ionization strengthens the water–base interaction. Just as the interaction energy of GC increased due to the presence of charge, the hydration energies also increase. In the major groove, $\Delta E_{HYD}$ of structure $\mathbf{1}^{\bullet-}$ is larger by 3.7 kcal $mol^{-1}$ than neutral structure **1**. $\Delta E_{HYD}$ of minor groove structures **2** and **3** both increase by 1.5 kcal $mol^{-1}$ upon ionization, while that of **4** increases by 3.5 kcal $mol^{-1}$. The presence of stack hydrates also indicates a stronger water–base interaction in the anionic trimer. The neutral GC–water interaction is insufficient to generate a minimum in the region above the GC plane at the B3LYP/DZP++ level of theory. Once a charge is introduced, water binds to the top plane of GC with $\Delta E_{HYD}$ of nearly 10.0 kcal $mol^{-1}$.

The charge distribution of $[GC{\cdot}H_2O]^{\bullet-}$ provides insight into the repercussions of NAB damage by identifying charged, chemically active regions. Table 4 lists the accumulation of

**Table 4. Negative Charge Distribution for Canonical and Proton-Transferred $[GC{\cdot}H_2O]^{\bullet-}$ Structures Are Given in Percentages of Total Charge Per Monomer**

| | guanine | cytosine | water |
|---|---|---|---|
| | Watson–Crick | | |
| major groove | | | |
| $\mathbf{1}^{\bullet-}$ | 14.9 | 82.2 | 2.9 |
| minor groove | | | |
| $\mathbf{2}^{\bullet-}$ | 13.8 | 80.7 | 5.5 |
| $\mathbf{3}^{\bullet-}$ | 13.6 | 80.9 | 5.5 |
| $\mathbf{4}^{\bullet-}$ | 12.3 | 83.0 | 4.7 |
| stack | | | |
| $\mathbf{5}^{\bullet-}$ | 14.9 | 82.5 | 2.6 |
| $\mathbf{6}^{\bullet-}$ | 14.4 | 81.0 | 4.6 |
| | Proton-Transferred | | |
| major groove | | | |
| **PT** $\mathbf{1}^{\bullet-}$ | 86.3 | 9.9 | 3.8 |
| minor groove | | | |
| **PT** $\mathbf{2}^{\bullet-}$ | 87.3 | 8.5 | 4.2 |
| **PT** $\mathbf{3}^{\bullet-}$ | 87.3 | 8.5 | 4.2 |
| **PT** $\mathbf{4}^{\bullet-}$ | 83.0 | 11.0 | 6.0 |

charge per molecule of both the Watson–Crick and proton-transferred forms. More details are provided on the proton-transferred monohydrates below. The percent negative charge on cytosine for the Watson–Crick structures varies from 80.7% to 83.0%. Regardless of how water interacts with $[GC]^{\bullet-}$, about 18% of the total charge flows from cytosine to either guanine or water due to noncovalent interactions. Approximately 3–5% of the charge is distributed to water, and the remaining is acquired by guanine. The distribution of charge among noncovalently bound molecules coincides with distinct changes in the hydration structure upon electron attachment.

Interbase proton transfer causes drastic changes in the molecular charge distribution. Once a proton migrates from guanine to cytosine, the percent negative charge on cytosine decreases from more than 80% to less than 11%. The majority of the negative charge is held by guanine (~85%), and water accounts for 4–6% of the charge. In many cases, DNA damage pathways involve reactive radical centers, which can be mutated via distonic processes. Here, hydration proves to alleviate a small percentage of the charge near the radical center, and proton-transfer provides clear separation of charge and spin.


dx.doi.org/10.1021/jp211608b | J. Phys. Chem. B 2012, 116, 5579–5587

**Proton-Transferred GC Monohydrates.** Interbase proton transfer results in a negatively charged, deprotonated guanine and a neutral cytosine radical. Comparing the VDEs of $[GC]^{\bullet-}$ and PT $[GC]^{\bullet-}$ reveals how proton transfer affects the nature of the unpaired electron. VDEs of $[GC]^{\bullet-}$ as well as AEAs of GC are listed in Table 5. VDEs and AEAs for both Watson–Crick and proton-transferred conformers are listed, including results for the proton-transferred $[GC]^{\bullet-}$ monohydrates. The VDE of canonical $[GC]^{\bullet-}$ is smaller than the proton-transferred analogue by 0.8 eV. This dramatic change in the VDE results from neutralizing the radical region, which lowers the energy of the PT $GC^{\bullet-}$. The monohydrates (Figures 4 and 5) undergo similar reductions in the VDE with respect to proton-transfer. The interaction with water increases the AEA of the guanine–cytsosine base pair by approximately 0.1 eV, and the trend is mimicked by the VDEs. The primary influence on the electronic properties of GC radical anion is the proton-transfer process. Noncovalent interactions have a smaller influence, indicated by modest changes in the VDE, AEA, and, congruently, the charge distribution.

**Table 5. Adiabatic Electron Affinities (AEA), Vertical Detachment Energies (VDE), and Vertical Detachment Energies of the Proton-Transferred Species (PT VDE) at the B3LYP/DZP++ Level of Theory**[a]

| | AEA (eV) | VDE (eV) | PT VDE (eV) |
|---|---|---|---|
| GC | 0.44 (0.60) | 1.21 | 2.03 |
| major groove | | | |
| **1** | 0.61 (0.76) | 1.37 | 2.22 |
| minor groove | | | |
| **2** | 0.52 (0.68) | 1.33 | 2.10 |
| **3** | 0.52 (0.68) | 1.33 | 2.12 |
| **4** | 0.55 (0.71) | 1.32 | 2.17 |
| stack | | | |
| **5** | 0.54 (0.68) | 1.43 | |
| **6** | 0.52 (0.68) | 1.49 | |

[a]Values in parentheses are the ZPVE-corrected AEAs. Proton-transferred analogues of the stack structures were not found.

Structures of $[GC{\cdot}H_2O]^{\bullet-}$ in which a proton has transferred from G(N1) to C(N3) are shown in Figures 4 and 5. Structures **PT 1**$^{\bullet-}$, **PT 2**$^{\bullet-}$, **PT 3**$^{\bullet-}$, and **PT 4**$^{\bullet-}$ are quite similar to the corresponding structures of the anionic Watson–Crick monohydrates. Although the charge distribution changes drastically upon proton transfer, the ESP felt by the interacting water molecule is relatively unchanged (Figure 3). Just as the ESP does not follow the unpaired electron, it does not follow local charges. However, $\Delta E_{HYD}$ of the proton-transferred species differ slightly from those of the Watson–Crick species (Table 3). Proton transfer strengthens the water–guanine interaction by about 2.0 kcal mol$^{-1}$, and the water–cytosine interaction weakens about 1.0 kcal mol$^{-1}$. Among all structures considered, that with the largest $\Delta E_{HYD}$ is structure **PT 1**$^{\bullet-}$. When generalizing the results presented here to electron attachment to DNA, the thermal product of electron attachment involves a distonic proton-transfer and a strong interaction with water in the major groove of DNA.

## CONCLUSIONS

At the heart of direct DNA damage via low-energy electron attachment is the physical nature of the radical species. Here, we report an array of physical properties for the monohydrated guanine–cytosine radical anion, including electron affinities, vertical detachment energies, spin densities, and charge distributions. Direct comparison of neutral and anionic guanine–cytosine monohydrates yields insight into the physical changes that take place upon ionization. Proton transfer in DNA subunits has become ubiquitous in the context of DNA damage, and our work demonstrates how proton-transfer lowers the energy of $[GC]^{\bullet-}$ and increases the electron affinity of GC in both isolated and monohydrated forms.

Structures of $[GC{\cdot}H_2O]^{\bullet-}$ and $[GC{\cdot}H_2O]$ are computed at the DZP++ B3LYP level of theory. We provide evidence that water interacts with the base pair, regardless of ionization state, within both the major groove and minor groove of DNA. Additional minima are identified for the anionic system in which water binds to the top plane of GC. Structures are also reported for the proton-transferred analogue of the GC radical anion, and minimal changes in the hydration structure are found with respect to proton transfer. Hydration energies for all three trimers are computed at the ZAPT2/aug-cc-pVDZ level of theory and include ZPVE effects. This work represents the first application of ZAPT2 theory to the $[GC]^{\bullet-}$ system and its monohydrates. Upon ionization, the proton-transferred conformation of $[GC]^{\bullet-}$ is energetically preferable to the Watson–Crick configuration, and water binds most strongly within the major groove.

The monohydrated guanine–cytosine base pair provides a good diagnostic system for the effects of electron attachment. Biological processes can be understood in greater detail when including neighboring molecules and noncovalent interactions in the model simulation. Although our results do not completely account for solvent effects, they reveal precisely how the presence of guanine and the interaction with a single water molecule alters the physical condition of the cytosine radical anion, a notorious species in the world of DNA damage.

## ASSOCIATED CONTENT

### Supporting Information

Cartesian coordinates and absolute energies for all species discussed in this article. This material is available free of charge via the Internet at http://pubs.acs.org.

## AUTHOR INFORMATION

### Corresponding Author

*E-mail: qc@uga.edu.

### Notes

The authors declare no competing financial interest.

## ACKNOWLEDGMENTS

A.G. thanks DST, Government of India, for a BOYSCAST Fellowship 2009–2010. This research was supported by the U.S. National Science Foundation, Grant CHE-1054286.

## REFERENCES

(1) Steenken, S.; Jovanovic, S. V. *J. Am. Chem. Soc.* **1997**, *119*, 617–618.

(2) Kumar, A.; Sevilla, M. D. In *Radiation Induced Molecular Phenomena in Nucleic Acids: A Comprehensive Theoretical and Experimental Analysis*; Shukla, M. K., Leszczynski, J., Eds.; Springer-Verlag: Berlin, Germany, 2008; Chapter 20, pp 577–617.

(3) Cadet, J.; Bellon, S.; Douki, T.; Frelon, S.; Gasparutto, D.; Muller, E.; Pouget, J.-P.; Ravanat, J.-L.; Romieu, A.; Sauvaigo, S. *J. Environ. Pathol. Toxicol. Oncol.* **2004**, *23*, 33–43.

(4) Wallace, S. S. *Free Radical Biol. Med.* **2002**, *33*, 1–14.

(5) Slupphaug, G.; Kavli, B.; Krokan, H. E. *Mutat. Res., Fundam. Mol. Mech. Mutagen.* **2003**, *531*, 231−251.
(6) Sonntag, C. *The Chemical Basis of Radiation Biology*; Taylor & Francis: Philadelphia, PA, 1987.
(7) Michael, B. D.; O'Neill, P. *Science* **2000**, *287*, 1603−1604.
(8) Cadet, J.; Delatour, T.; Douki, T.; Gasparutto, D.; Ravanat, J.-L.; Sauvaigo, S. *Mutat. Res., Fundam. Mol. Mech. Mutagen.* **1999**, *424*, 9−21.
(9) Cobut, V.; Frongillo, Y.; Patau, J. P.; Goulet, T.; Fraser, M.-J.; Jay-Gerin, J.-P. *Radiat. Phys. Chem.* **1998**, *51*, 229−243.
(10) Pimblott, S. M.; LaVerne, J. A. In *Radiation Damage in DNA: Structure/Function Relationships at Early Times*; Fuciarelli, A. F., Zimbrick, J. D., Eds.; Battelle Press: Columbus, OH, 1995; pp 3−12.
(11) Srdoc, D.; Inokuti, M.; Kracjar-Broni, C. In *IAEA CRP Atomic and Molecular Data for Radiotherapy and Radiation Research*; Inokuti, M., Ed.; IAEA: Vienna, Austria, 1995.
(12) Steenken, S.; Telo, J. P.; Novais, H. M.; Candeias, L. P. *J. Am. Chem. Soc.* **1992**, *114*, 4701−4709.
(13) Becker, D.; Sevilla, M. D. *Advances in Radiation Biology*; Academic Press: New York, 1993.
(14) Kelley, S. O.; Barton, J. K. *Science* **1999**, *283*, 375−381.
(15) Hall, D. B.; Holmlin, R. E.; Barton, J. K. *Nature* **1996**, *382*, 731−735.
(16) Fink, H.-W.; Schönenberger, C. *Nature* **1999**, *398*, 407−410.
(17) Steenken, S. *Biol. Chem.* **1997**, *378*, 1292−1297.
(18) Berlin, Y. A.; Burin, A. L.; Ratner, M. A. *J. Am. Chem. Soc.* **2001**, *123*, 260−268.
(19) Fink, H.-W. *Cell. Mol. Life Sci.* **2001**, *58*, 1−3.
(20) Robertson, N.; McGowan, C. A. *Chem. Soc. Rev.* **2003**, *32*, 96−103.
(21) Boudaïffa, B.; Cloutier, P.; Hunting, D.; Huels, M. A.; Sanche, L. *Science* **2000**, *287*, 1658−1660.
(22) Sanche, L. *Eur. Phys. J. D* **2005**, *35*, 367−390.
(23) Simons, J. *Acc. Chem. Res.* **2006**, *39*, 772−779.
(24) Ray, S. G.; Daube, S. S.; Naaman, R. *Proc. Natl. Acad. Sci. U.S.A.* **2005**, *102*, 15−19.
(25) Li, X.; Sevilla, M. D.; Sanche, L. *J. Am. Chem. Soc.* **2003**, *125*, 13668−13669.
(26) Ptasińska, S.; Denifl, S.; Gohlke, S.; Scheier, P.; Illenberger, E.; Märk, T. D. *Angew. Chem., Int. Ed.* **2006**, *45*, 1893−1896.
(27) Gu, J.; Xie, Y.; Schaefer, H. F. *J. Am. Chem. Soc.* **2006**, *128*, 1250−1252.
(28) Gu, J.; Wang, J.; Leszczynski, J. *J. Am. Chem. Soc.* **2006**, *128*, 9322−9323.
(29) Ratner, M. *Nature* **1999**, *397*, 480−481.
(30) Taubes, G. *Science* **1997**, *275*, 1420−1421.
(31) Wetmore, S. D.; Boyd, R. J.; Eriksson, L. A. *Chem. Phys. Lett.* **2000**, *322*, 129−135.
(32) Harańczyk, M.; Gutowski, M. *J. Am. Chem. Soc.* **2005**, *127*, 699−706.
(33) Bachorz, R. A.; Rak, J.; Gutowski, M. *Phys. Chem. Chem. Phys.* **2005**, *7*, 2116−2125.
(34) Harańczyk, M.; Rak, J.; Gutowski, M. *J. Chem. Phys. A* **2005**, *109*, 11495−11503.
(35) Mazurkiewicz, K.; Bachorz, R. A.; Gutowski, M.; Rak, J. *J. Phys. Chem. B* **2006**, *110*, 24696−24707.
(36) Bachorz, R. A.; Klopper, W.; Gutowski, M. *J. Chem. Phys.* **2007**, *126*, 085101.
(37) Harańczyk, M.; Gutowski, M.; Li, X.; Bowen, K. H. *Proc. Natl. Acad. Sci. U.S.A.* **2007**, *104*, 4804−4807.
(38) Chen, E. C. M.; Chen, E. S. *J. Phys. Chem. B* **2000**, *104*, 7835−7844.
(39) Desfrançois, C.; Periquet, V.; Bouteiller, Y.; Schermann, J. P. *J. Phys. Chem. A* **1998**, *102*, 1274−1278.
(40) Wesolowski, S. S.; Leininger, M. L.; Pentchev, P. N.; Schaefer, H. F. *J. Am. Chem. Soc.* **2001**, *123*, 4023−4028.
(41) Li, X.; Cai, Z.; Sevilla, M. D. *J. Phys. Chem. B* **2001**, *105*, 10115−10123.
(42) Li, X.; Cai, Z.; Sevilla, M. D. *J. Phys. Chem. A* **2002**, *106*, 9345−9351.
(43) Reynisson, J.; Steenken, S. *Phys. Chem. Chem. Phys.* **2002**, *4*, 5353−5358.
(44) Richardson, N. A.; Wesolowski, S. S.; Schaefer, H. F. *J. Am. Chem. Soc.* **2002**, *124*, 10163−10170.
(45) Richardson, N. A.; Wesolowski, S. S.; Schaefer, H. F. *J. Phys. Chem. B* **2003**, *107*, 848−853.
(46) Kumar, A.; Knapp-Mohammady, M.; Mishra, P. C.; Suhai, S. *J. Comput. Chem.* **2004**, *25*, 1047−1059.
(47) Richardson, N. A.; Gu, J.; Wang, S.; Xie, Y.; Schaefer, H. F. *J. Am. Chem. Soc.* **2004**, *126*, 4404−4411.
(48) Abo-Riziq, A.; Grace, L.; Nir, E.; Kabelac, M.; Hobza, P.; de Vries, M. S. *Proc. Natl. Acad. Sci. U.S.A.* **2005**, *102*, 20−23.
(49) Hendricks, J. H.; Lyapustina, S. A.; de Clercq, H. L.; Snodgrass, J. T.; Bowen, K. H. *J. Chem. Phys.* **1996**, *104*, 7788−7791.
(50) Hendricks, J. H.; Lyapustina, S. A.; de Clercq, H. L.; Bowen, K. H. *J. Chem. Phys.* **1998**, *108*, 8−11.
(51) Schiedt, J.; Weinkauf, R.; Neumark, D. M.; Schlag, E. W. *Chem. Phys.* **1998**, *239*, 511−524.
(52) Li, X.; Bowen, K. H.; Haranczyk, M.; Bachorz, R.; Mazurkiewicz, K.; Rak, J.; Gutowski, M. *J. Chem. Phys.* **2007**, *127*, 174309.
(53) Eustis, S.; Wang, D.; Lyapustina, S.; Bowen, K. H. *J. Chem. Phys.* **2007**, *127*, 224309.
(54) Aflatooni, K.; Gallup, G. A.; Burrow, P. D. *J. Phys. Chem. A* **1998**, *102*, 6205−6207.
(55) Desfrançois, C.; Abdoul-Carime, H.; Schermann, J. P. *J. Chem. Phys.* **1996**, *104*, 7792.
(56) Periquet, V.; Moreau, A.; Carles, S.; Schermann, J. P.; Desfrançois, C. *J. Electron Spectrosc. Relat. Phenom.* **2000**, *106*, 141−151.
(57) Hanel, G.; Gstir, B.; Denifl, S.; Scheier, P.; Probst, M.; Farizon, B.; Farizon, M.; Illenberger, E.; Märk, T. D. *Phys. Rev. Lett.* **2003**, *90*, 188104.
(58) Denifl, S.; Ptasinska, S.; Cingel, M.; Matejcik, S.; Scheier, P.; Märk, T. D. *Chem. Phys. Lett.* **2003**, *377*, 74−80.
(59) Abdoul-Carime, H.; Gohlke, S.; Illenberger, E. *Phys. Rev. Lett.* **2004**, *92*, 168103.
(60) Sevilla, M. D.; Becker, D.; Yan, M.; Summerfield, S. R. *J. Phys. Chem.* **1991**, *95*, 3409−3415.
(61) Szyperska, A.; Rak, J.; Leszczynski, J.; Li, X.; Ko, Y. J.; Wang, H.; Bowen, K. H. *J. Am. Chem. Soc.* **2009**, *131*, 2663−2669.
(62) Radisic, D.; Bowen, K. H.; Dabkowska, I.; Storoniak, P.; Rak, J.; Gutowski, M. *J. Am. Chem. Soc.* **2005**, *127*, 6443−6450.
(63) Szyperska, A.; Rak, J.; Leszczynski, J.; Li, X.; Ko, Y. J.; Wang, H.; Bowen, K. H. *ChemPhysChem* **2010**, *11*, 880−888.
(64) Yates, B. F.; Bouma, W. J.; Radom, L. *J. Am. Chem. Soc.* **1984**, *106*, 5805−5808.
(65) Yates, B. F.; Bouma, W. J.; Radom, L. *Tetrahedron* **1986**, *42*, 6225−6234.
(66) Löwdin, P.-O. *Rev. Mod. Phys.* **1963**, *35*, 724−732.
(67) Löwdin, P.-O. *Adv. Quantum Chem.* **1966**, *2*, 213−360.
(68) Wagenknecht, H.-A. *Angew. Chem., Int. Ed.* **2003**, *42*, 2454−2460.
(69) Ito, T.; Rokita, S. E. *Angew. Chem., Int. Ed.* **2004**, *43*, 1839−1842.
(70) Ghosh, A. K.; Schuster, G. B. *J. Am. Chem. Soc.* **2006**, *128*, 4172−4173.
(71) Dabkowska, I.; Rak, J.; Gutowski, M. *Eur. Phys. J. D* **2005**, *35*, 429−435.
(72) Gu, J.; Wang, J.; Rak, J.; Leszczynski, J. *Angew. Chem., Int. Ed.* **2007**, *46*, 3479−3481.
(73) Sobolewski, A. L.; Domcke, W. *Phys. Chem. Chem. Phys.* **2004**, *6*, 2763−2771.
(74) Sobolewski, A. L.; Domcke, W.; Hättig, C. *Proc. Natl. Acad. Sci. U.S.A.* **2005**, *102*, 17903−17906.
(75) Perun, S.; Sobolewski, A. L.; Domcke, W. *J. Phys. Chem. A* **2006**, *110*, 9031−9038.

(76) Schwalb, N. K.; Temps, F. *J. Am. Chem. Soc.* **2007**, *129*, 9272−9273.
(77) Kumar, A.; Sevilla, M. D. *Chem. Rev.* **2010**, *110*, 7002−7023.
(78) Kumar, A.; Sevilla, M. D. *J. Phys. Chem. B* **2009**, *113*, 11359−11361.
(79) Rejnek, J.; Hanus, M.; Kabelàč, M.; Ryjàček, F.; Hobza, P. *Phys. Chem. Chem. Phys.* **2005**, *7*, 2006−2017.
(80) Makarov, V.; Pettitt, B. M.; Feig, M. *Acc. Chem. Res.* **2002**, *35*, 376−384.
(81) Barciszewski, J.; Jurczak, J.; Porowski, S.; Specht, T.; Erdmann, V. A. *Eur. J. Biochem.* **1999**, *260*, 293−307.
(82) Auffinger, P.; Westhof, E. *J. Mol. Biol.* **2000**, *300*, 1113−1131.
(83) Orozoco, M.; Luque, F. J. *Biopolymers* **1993**, *33*, 1851−1869.
(84) Colson, A. O.; Besler, B.; Sevilla, M. D. *J. Phys. Chem.* **1993**, *97*, 13852−13859.
(85) Sevilla, M. D.; Besler, B.; Colson, A. O. *J. Phys. Chem.* **1994**, *98*, 2215.
(86) Bao, X.; Sun, H.; Wong, N.-B.; Gu, J. *J. Phys. Chem. B* **2006**, *110*, 5865−5874.
(87) Bao, X.; Liang, G.; Wong, N.-B.; Gu, J. *J. Phys. Chem. A* **2007**, *111*, 666−672.
(88) Kumar, A.; Sevilla, M. D.; Suhai, S. *J. Phys. Chem. B* **2008**, *112*, 5189−5198.
(89) Nugent, M. L.; Adamowicz, L. *Mol. Phys.* **2005**, *103*, 1467−1472.
(90) Kim, S.; Schaefer, H. F. *J. Chem. Phys.* **2007**, *126*, 064301.
(91) Kim, S.; Schaefer, H. F. *J. Chem. Phys.* **2010**, *133*, 144305.
(92) Chen, H.-Y.; Kao, C.-L.; Hsu, S. C. N. *J. Am. Chem. Soc.* **2009**, *131*, 15930−15938.
(93) Chen, H.-Y.; Hsu, S. C. N.; Kao, C.-L. *Phys. Chem. Chem. Phys.* **2010**, *12*, 1253−1263.
(94) Becke, A. D. *J. Chem. Phys.* **1993**, *98*, 5648−5652.
(95) Lee, C.; Yang, W.; Parr, R. G. *Phys. Rev. B* **1988**, *37*, 785−789.
(96) Huzinaga, S. *J. Chem. Phys.* **1965**, *42*, 1293−1302.
(97) Dunning, T. H. *J. Chem. Phys.* **1970**, *53*, 2823−2833.
(98) Lee, T. J.; Schaefer, H. F. *J. Chem. Phys.* **1985**, *83*, 1784−1794.
(99) Rienstra-Kiracofe, J. C.; Tschumper, G. S.; Schaefer, H. F.; Nandi, S.; Ellison, G. B. *Chem. Rev.* **2002**, *102*, 231−282.
(100) Jaeger, H. M.; Schaefer, H. F. *J. Phys. Chem. B* **2009**, *113*, 8142−8148.
(101) Kim, N. J.; Kim, Y. S.; Jeong, G.; Ahn, T. K.; Kim, S. K. *Int. J. Mass. Spectrom.* **2002**, *219*, 11−21.
(102) Jayatilaka, D.; Lee, T. J. *Chem. Phys. Lett.* **1992**, *199*, 211−219.
(103) Lee, T. J.; Jayatilaka, D. *Chem. Phys. Lett.* **1993**, *201*, 1−10.
(104) Jayatilaka, D.; Lee, T. J. *J. Chem. Phys.* **1993**, *98*, 9734−9747.
(105) Lee, T. J.; Rendell, A. P.; Dyall, K. G.; Jayatilaka, D. *J. Chem. Phys.* **1994**, *100*, 7400−7409.
(106) Wheeler, S. E.; Allen, W. D.; Schaefer, H. F. *J. Chem. Phys.* **2008**, *128*, 0741070.
(107) Dunning, T. H. *J. Chem. Phys.* **1989**, *90*, 1007−1023.
(108) Kendall, R. A.; Dunning, T. H.; Harrison, R. J. *J. Chem. Phys.* **1992**, *96*, 6796−6806.
(109) Kawahara, S.-I.; Uchimaru, T. *Phys. Chem. Chem. Phys.* **2000**, *2*, 2869−2872.
(110) Riley, K. E.; Hobza, P. *J. Phys. Chem. A* **2007**, *111*, 8257−8263.
(111) Reed, A. E.; Weinhold, F. A.; Curtiss, L. A.; Pochatko, D. J. *J. Chem. Phys.* **1986**, *84*, 5687−5705.
(112) Reed, A. E.; Weinhold, F. A. *J. Chem. Phys.* **1983**, *78*, 4066−4073.
(113) Foster, J. P.; Weinhold, F. A. *J. Am. Chem. Soc.* **1980**, *102*, 7211−7218.
(114) Reed, A. E.; Weinstock, R. B.; Weinhold, F. A. *J. Chem. Phys.* **1985**, *83*, 735−746.
(115) Weinhold, F. A. In *Encyclopedia of Computational Chemistry*; von Ragué Schleyer, P., Allinger, N. L., Clark, T., Gasteiger, J., Kollman, P. A., Schaefer, H. F., Schreiner, P. R., Eds.; John Wiley and Sons, Ltd.: New York, 1998; Vol. 3, pp 1792−1811.
(116) Shao, Y.; et al. *Phys. Chem. Chem. Phys.* **2006**, *8*, 3172−3191.